

# Accepted Manuscript

Research paper

Structure, thermal stability, antioxidant activity and DFT studies of trisphenols and related phenols

Shasha Yu, Yishan Wang, Yujie Ma, Limin Wang, Jia Zhu, Shenggao Liu

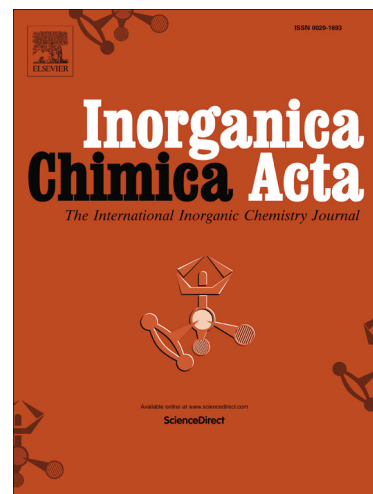
PII: S0020-1693(17)30194-9  
DOI: <http://dx.doi.org/10.1016/j.ica.2017.07.022>  
Reference: ICA 17745

To appear in: *Inorganica Chimica Acta*

Received Date: 16 February 2017  
Revised Date: 19 June 2017  
Accepted Date: 3 July 2017

Please cite this article as: S. Yu, Y. Wang, Y. Ma, L. Wang, J. Zhu, S. Liu, Structure, thermal stability, antioxidant activity and DFT studies of trisphenols and related phenols, *Inorganica Chimica Acta* (2017), doi: <http://dx.doi.org/10.1016/j.ica.2017.07.022>

This is a PDF file of an unedited manuscript that has been accepted for publication. As a service to our customers we are providing this early version of the manuscript. The manuscript will undergo copyediting, typesetting, and review of the resulting proof before it is published in its final form. Please note that during the production process errors may be discovered which could affect the content, and all legal disclaimers that apply to the journal pertain.



# Structure, thermal stability, antioxidant activity and DFT studies of trisphenols and related phenols

Shasha Yu <sup>a</sup>, Yishan Wang <sup>b</sup>, Yujie Ma <sup>a</sup>, Limin Wang <sup>c</sup>, Jia Zhu <sup>b,\*</sup>, Shenggao Liu<sup>a,\*</sup>

<sup>a</sup> Polymers and composites division, Ningbo Institute of Materials Technology and Engineering, Chinese Academy of Sciences, Ningbo 315201, China

<sup>b</sup> College of Chemistry, Beijing Normal University, Beijing 100875, China

<sup>c</sup> School of Chemical Engineering and Environment, North University of China, Taiyuan 030051, China

**Abstract:** Two kinds of trisphenols have been successfully synthesized and their structures were confirmed by IR spectra, <sup>1</sup>HNMR, <sup>13</sup>CNMR, mass spectra and X-ray diffraction. They exhibited better thermal stability than both monophenol and bisphenols due to their higher molecular weight. Moreover, their antioxidant activities have been investigated in lubricant oil using PDSC and RBOT. The results showed that the *o*-trisphenol **3b** exhibited the best antioxidant activity while the *p*-trisphenol **3a** was the worst. In addition, their relationship between structures and properties has been further explored by a series of DFT calculations including the BDE values, the IP values and the Gibbs free energy barriers for the reaction between phenols and methylperoxyl radicals.

**Keywords:** Antioxidant activity; Trisphenol; Thermal stability; Lubricant; DFT

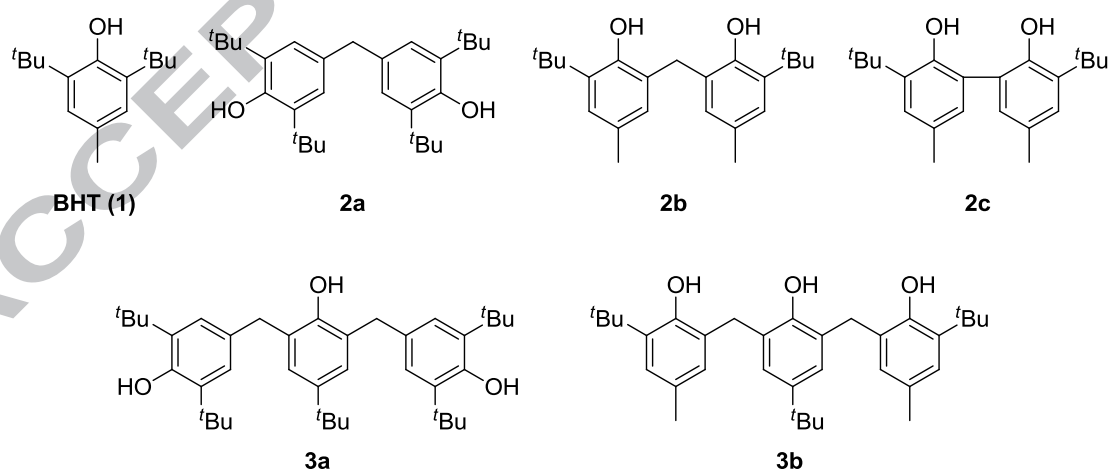
## 1. Introduction

Phenols (especially the sterically hindered phenols) have been used as antioxidants in a wide variety of industrial applications such as rubber processing, plastic resins, fuel and lubricants, and others since they are always low-toxic, highly effective, non-discoloring and eco-friendly [1-2]. A market research published by BCC Research reported that the substituted phenols category should account for 35.6% market share and the total market would reach to \$ 1.92 billion at a five-year compound annual growth rate (CAGR) of 5.0% by 2019 which is the fastest growing rate of all the antioxidants [3]. 2,6-di-*tert*-butyl-4-methylphenol (**BHT**, **1**) employed from 1937 is the most frequently used antioxidant recognized as safe for application in foods and industry [4-5]. In fact, it is unfavorable for the modern materials or machines which need to be operated at elevated temperatures ascribed to the poor thermal stability and antioxidant efficiency [6-7]. For example, the working temperature of the aircraft engines is already above 200 °C while the initial decomposition temperature is only 88 °C [8-9]. Hence, to design and develop novel antioxidants with superior performance at high temperatures is becoming an urgent project.

In this regard, bisphenols with two phenolic groups in one molecule have gained a wide range of attention in academia and industry owing to their higher antioxidant performance and improved thermal stability. [10-15]. For example, the reactivity toward peroxy radicals of *o*-bisphenol (6,6'-methylenebis(2-(*tert*-butyl)-4-methylpheno, **2b**) is nearly 61-fold and 65-fold higher than that of BHT and *p*-bisphenol (4,4'-methylenebis(2,6-di-*tert*-butylphenol, **2a**) respectively on account of the less bulky substitutes and the larger stabilization of the formed phenoxyl radical of **2b** [10]. However, as for the similar compound *o*-bisphenol (3,3'-di-*tert*-butyl-5,5'-dimethyl-[1,1'-biphenyl]-2,2'-diol, **2c**) which the two phenols are directly connected, the reactivity is practically far poorer than that of **2b** and nearly identical to that of BHT since the formation of a twin intramolecular hydrogen bond in the starting phenol largely reduces the activity of the O-H groups [11]. It clearly demonstrates that the relative position of the two OH groups and the

linking group that connected them exert the most significant influence on the antioxidant efficiency. Although not all the bisphenols exhibit better antioxidant performance than BHT, their thermal stabilities have got significantly improved since some of them such as **2a** and **2b** have already been applied in the industry instead.

These reports aroused our interest to investigate the properties of the trisphenols which are composed of three phenolic moieties. First, the obviously increased molecular weight can theoretically improve their thermal stability at elevated temperatures [9]. Second, considering the delicate influence of the structures on the performance of bisphenols, developing highly efficient antioxidants of trisphenols is feasible through designing the reasonable structures. Consequently, based on the previous reports, we have synthesized two kinds of trisphenols (**3a** and **3b**) which the aromatic rings are bridged by two methylene groups at different linking positions. In this paper, other structurally related phenols including monophenol (**1**) and bisphenols (**2a** and **2b**) were also considered to further evaluate the properties of the trisphenols (Scheme 1). Moreover, a series of DFT calculations were provided to investigate the relationship between the structures and the properties which will be beneficial for the future design of phenolic antioxidants.



**Scheme 1.** The structures of trisphenols and the related phenols.

## 2. Experimental

### 2.1. Materials

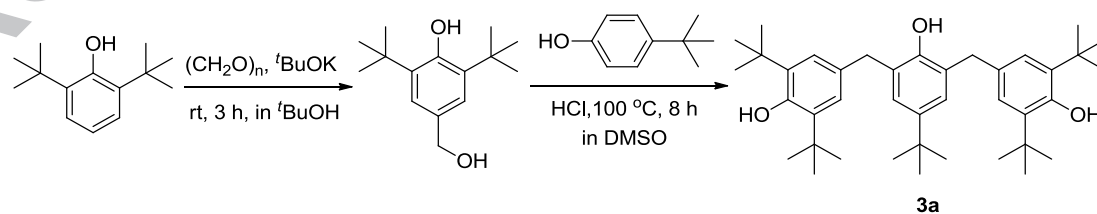
BHT and silica gel for column chromatography were purchased from Sinopharm Chemical Reagent Co., Ltd. 4,4'-methylenebis(2,6-di-*tert*-butylphenol) was procured from TCI Company. 6,6'-methylenebis(2-(*tert*-butyl)-4-methylphenol) was purchased from Energy Chemical Company (Shanghai, China). 150SN was obtained from China National Petroleum Corporation. 150N was supplied by China National Offshore Oil Corporation. YUBASE was purchased from SK Corporation (South Korea). PAO was provided from INEOS (England).

## 2.2. Characterization

All  $^1\text{H}$  and  $^{13}\text{C}$  NMR spectra were recorded at room temperature in  $\text{CDCl}_3$  (containing 0.03% TMS) or in  $\text{DMSO-}d_6$  on Bruker AV/ANCE-400 MHz spectrometer.  $^1\text{H}$  NMR spectra was recorded with tetramethylsilane ( $\delta = 0.00$  ppm) or the residual solvent peak of  $\text{DMSO-}d_6$  ( $\delta = 2.50$  ppm);  $^{13}\text{C}$  NMR spectra was recorded with  $\text{CDCl}_3$  ( $\delta = 77.00$  ppm) or the residual solvent peak of  $\text{DMSO-}d_6$  ( $\delta = 39.52$  ppm) as internal reference. High-resolution mass spectra were obtained by using Waters Micromass GCT or Agilent Technologies 6224 TOF LC/MS mass spectrometers. IR spectra were obtained by using a Thermo-fisher 6700 spectrometer. Single crystal X-ray diffraction data were collected at 293(2) K for **2a** and **2b** on Bruker SMART diffractometer, 130 K for **3a** and **3b** on Bruker APEX-II diffractometer.

## 2.3. Synthesis

### Synthesis Process and Structural Characterization of trisphenol **3a**.



**Scheme 2.** Synthesis process of **3a**

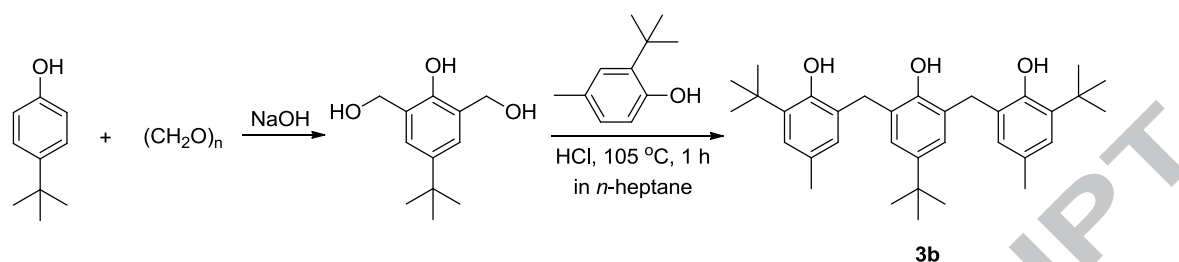
Trisphenol **3a** was prepared with two steps by the route schematically shown in Scheme 2.

**1) Synthesis of 2,6-di-*tert*-butyl-4-(hydroxymethyl)phenol**

Paraformaldehyde (364 mmol, 10.91 g), *t*BuOK (14.5 mmol, 1.63 g) and *t*BuOH (300 mL) were placed in a 500 mL round-bottomed flask. The flask was heated in an oil bath at 70 °C under an inert atmosphere until the paraformaldehyde has been completely depolymerized. After cooling to room temperature, 2,6-di-*tert*-butylphenol (145.4 mmol, 30 g) was added and the obtained mixture was stirred at room temperature for 3 h. Then 200 mL of water was added to quench the reaction. The mixture was extracted with ethyl acetate, and the extract was washed with brine. The organic layer was dried over anhydrous Na<sub>2</sub>SO<sub>4</sub>. The solvent was evaporated in vacuo and the residue was purified by column chromatography on 230-400 mesh of silica gel (petroleum ether/ethyl acetate = 10/1) to afford **2,6-di-*tert*-butyl-4-(hydroxymethyl)phenol** as a white solid in 73% yield (34.4 g). <sup>1</sup>H NMR (400 MHz, CDCl<sub>3</sub>) δ (ppm) 1.45 (singlet, 18H), 3.53 (broad, 1 H), 4.60 (singlet, 2H), 5.23 (singlet, 1H), 7.19 (singlet, 2H).

**2) Synthesis of compound 3a**

HCl (37%, 33.3 mL) was added to a solution of 4-(*tert*-butyl)phenol (12.6 mmol, 1.90 g) and 2,6-di-*tert*-butyl-4-(hydroxymethyl)phenol (25.4 mmol, 6.00 g) in DMSO (150 mL). The reaction mixture was stirred at 100 °C for 8 h in a pressure bottle. Then 200 mL of water was added to quench the reaction. The mixture was extracted with ethyl acetate, and the extract was washed with brine. The organic layer was dried over anhydrous Na<sub>2</sub>SO<sub>4</sub>. The solvent was evaporated in vacuo and the residue was purified by column chromatography on 230-400 mesh of silica gel (petroleum ether/toluene = 5/1) to afford the product as a light yellow solid in 68% yield (5.08 g). <sup>1</sup>H NMR (400 MHz, CDCl<sub>3</sub>) δ 1.27 (singlet, 9H), 1.37 (singlet, 36H), 3.88 (singlet, 4H), 4.63 (singlet, 1H), 5.05 (singlet, 2H), 7.01 (singlet, 4H), 7.04 (singlet, 2H). <sup>13</sup>C NMR (100 MHz, CDCl<sub>3</sub>) δ 30.4, 31.7, 34.2, 34.5, 36.8, 125.3, 126.1, 127.0, 130.5, 136.2, 143.0, 150.1, 152.4. IR (cm<sup>-1</sup>): 501, 531, 611, 673, 754, 768, 794, 912, 878, 11047, 1121, 1149, 1169, 1209, 1231, 1250, 1316, 1361, 1390, 1431, 1482, 2868, 2962, 3004, 3558, 3622, 3646. HRMS (ESI) calcd for C<sub>40</sub>H<sub>62</sub>NO<sub>3</sub> [M+NH<sub>4</sub>]<sup>+</sup>: 604.4724, found 604.4723. The structure of **3a** was determined by X-ray single-crystal analysis.

**Synthesis Process and Structural Characterization of trisphenol 3b.****Scheme 3.** Synthesis process of **3b**

Trisphenol **3b** was prepared with two steps by the route schematically shown in Scheme 3.

**1) Synthesis of (5-(tert-butyl)-2-hydroxy-1,3-phenylene)dimethanol**

4-(tert-butyl)phenol (20 mmol, 3.0 g) was added to an aqueous 4% NaOH solution (24 mL) and the mixture stirred at 50 °C to dissolve the starting material. After cooling to room temperature, 37% HCHO solution (5.5 mL) was added and the obtained mixture was stirred for 3 days. Then concentrated HCl (2.5 mL) was added to quench the reaction. The mixture was extracted with chloroform, and the extract was washed with water and brine. The organic layer was dried over anhydrous MgSO<sub>4</sub>. The solvent was evaporated in vacuo and the residue was purified by column chromatography on 230-400 mesh of silica gel (petroleum ether/ethyl acetate = 5/3) to afford (5-(tert-butyl)-2-hydroxy-1,3-phenylene)dimethanol as a colorless oil in 97% yield (4.08 g). <sup>1</sup>H NMR (400 MHz, CDCl<sub>3</sub>) δ (ppm) 1.27 (singlet, 9H), 2.52 (broad, 2H), 4.80 (singlet, 4H), 7.08 (singlet, 2H), 7.90 (broad, 1H).

**2) Synthesis of 3b**

To a solution of (5-(tert-butyl)-2-hydroxy-1,3-phenylene)dimethanol (18.5 mmol, 3.90 g) in *n*-heptane, 2-(tert-butyl)-4-methylphenol (130 mmol, 21.36 g) was added and the mixture was heated until homogeneous. Then 1 mL of concentrated hydrochloric acid was added and the mixture was heated at reflux for 1 h using a Dean Stark trap to remove water. After cooling to the room temperature, the mixture was extracted with ethyl acetate, and the extract was washed with brine. The organic layer was dried over anhydrous Na<sub>2</sub>SO<sub>4</sub>. The solvent was evaporated in vacuo and the

residue was purified by column chromatography on 230-400 mesh of silica gel (petroleum ether/ethyl acetate = 10/1) to afford the product as a light yellow solid in 56% yield (5.21 g).  $^1\text{H}$  NMR (400 MHz,  $\text{DMSO-}d_6$ )  $\delta$  1.12 (singlet, 9H), 1.34 (singlet, 18H), 2.09 (singlet, 6H), 3.85 (singlet, 4H), 6.62 (singlet, 2H), 6.81 (singlet, 2H), 6.90 (singlet, 2H), 8.11 (singlet, 2H), 8.84 (singlet, 1H).  $^{13}\text{C}$  NMR (100 MHz,  $\text{DMSO-}d_6$ )  $\delta$  20.9, 30.0, 31.0, 31.5, 33.8, 34.8, 125.1, 125.2, 127.0, 127.8, 128.2, 128.7, 137.0, 142.2, 149.3, 150.8. IR ( $\text{cm}^{-1}$ ): 611, 638, 764, 791, 858, 878, 1131, 1153, 1206, 1241, 1288, 1315, 1375, 1453, 1484, 2868, 2957, 3316, 3372, 3583. HRMS (ESI) calcd for  $\text{C}_{34}\text{H}_{50}\text{NO}_3$   $[\text{M}+\text{NH}_4]^+$ : 520.3785, found 520.3781. The structure of **3b** was determined by X-ray single-crystal analysis.

#### 2.4 Thermogravimetric analysis (TGA).

Thermogravimetric Analysis was conducted on a TGA Q500 (TA Instruments, Newcastle, DE, U.S.A.). Samples ( $5 \pm 0.5$  mg) were heated on a platinum pan from room temperature to 500 °C at a rate of 10.0 °C/min under a nitrogen atmosphere of flow 60.0 mL/min for the thermal stability experiments, and 700 °C at a rate of 10.0 °C/min under a compressed air of flow 60.0 mL/min for the thermo-oxidative stability experiments. Data were analyzed using TA Universal Analysis software, version 4.5A (TA Instruments, New Castle, DE, USA). The characteristic weight loss temperatures comprised of the onset of weight loss temperature ( $T_{\text{ON}}$ ) and the temperature at which the maximum rate of decomposition occurred ( $T_{\text{max}}$ ).  $T_{\text{ON}}$  was derived from the TGA plots and taken as the temperature at which 5% weight loss occurred ( $T_{\text{ON}, 5\%}$ ).  $T_{\text{max}}$  was taken as the peak maxima temperature from the corresponding DTG curves.

#### 2.5 Isothermal PDSC.

$3.0 \pm 0.2$  mg of oil sample was placed in a hermetically sealed aluminum pan with a pinhole lid for interaction of the sample with the reactant gas (high-purity oxygen). Oil samples were heated from 50 °C to the test temperature at a heating rate of 50 °C/min before being held in an isothermal mode. After two minutes of heat preservation, the oxygen (flow of 100 mL/min) was added in until the pressure was 3.5 MPa. When an exothermic peak of oxidation appeared, the test was finished.

Oxidation induction time (OIT) was measured from the start of the oxygen added in to the start of the exothermic peak.

## 2.6 Oxidation Stability using RBOT.

The method uses  $55.6 \pm 0.3$  g of oil with 5.0 ml of reagent water in the presence of copper catalyst at 150 °C. In RBOT, the vessel was charged with oxygen to 620.5 kPa pressure and rotated axially in a constant temperature at 150 °C. The pressure in the bomb was recorded with time, and the RBOT time is the time at which the maximum pressure of the bomb has dropped by 175.1 kPa. All oil samples were run in duplicate, and the average RBOT times were reported.

## 2.7 DFT study

All calculations were performed using the Gaussian 09 program package [16]. And the program, GaussianView [17], was used for visualization of molecular structures.

### 2.7.1 Calculation of BDE and IP

BDE and IP were calculated in gas-phase and *n*-hexane (the solvent which was performed in the experiment). Geometrical optimizations and vibrational frequencies consisting of molecules Ar-OH, Ar-O<sup>•</sup> and Ar-O<sup>•+</sup> were performed using B3LYP / 6-31 G (d, p) and single-point calculations at the level of M06-2X / 6-311+G (d, p) at 25 °C in vacuum and in *n*-hexane, respectively. Solvent contribution was performed employing IEF-PCM method [18]. Besides, each optimized structures were confirmed to be real minima by frequency analysis ( $N_{\text{imag}} = 0$ ). Furthermore, in terms of the computation of BDE, all possible isomeric phenolic radical forms were calculated and the most stable isomers were selected for further consideration.

BDE can be calculated using following equation:

$$\text{BDE} = H(\text{Ar-O}^{\bullet}) + H(\text{H}^{\bullet}) - H(\text{Ar-OH}),$$

where  $H(\text{Ar-O}^{\bullet})$  is the enthalpy of phenolic radical generated after H<sup>•</sup> abstraction,  $H(\text{H}^{\bullet})$  is the enthalpy of H atom, and  $H(\text{Ar-OH})$  is the enthalpy of phenol.

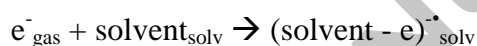
IP can be calculated by the equation:

$$\text{IP} = H(\text{Ar-O}^{\bullet+}) + H(\text{e}^{-}) - H(\text{Ar-OH}),$$

where  $H(\text{Ar-O}^{\bullet+})$  is the enthalpy of phenolic radical cation,  $H(\text{e}^{-})$  is the enthalpy of

electron.

The value for gas-phase enthalpy of hydrogen atom is -0.5 hartree [19]. Gas-phase enthalpy of electron is 3.145 kJ•mol<sup>-1</sup> [20]. For the solvation enthalpy of the hydrogen atom in *n*-hexane, where experimental value was not available, we used the average value  $\Delta_{\text{solv}}H(\text{H}^\bullet) = 5 \text{ kJ}\cdot\text{mol}^{-1}$ , because in organic solvents  $\Delta_{\text{solv}}H(\text{H}^\bullet) \approx \Delta_{\text{solv}}H(\text{H}_2)$  varies in very narrow (5±1) kJ•mol<sup>-1</sup> range [21-23]. For the solvation enthalpy of electron which was not available in *n*-hexane, it was performed at IEF-PCM/B3LYP/6-311++G (d, p) method which proved to be a relatively robust method when calculating solvation enthalpies of electron and proton [24-26]. And the enthalpy changes in the process as follows:



where  $\text{solvent}_{\text{solv}}$  is the molecule of solvent in the same solvent, and  $(\text{solvent} - e^-)_{\text{solv}}$  means that electron is attached to the molecule of solvent.

Then, the solvation enthalpy of electron is given by following equation:

$$\Delta_{\text{solv}}H(e^-) = H(\text{solvent} - e^-)_{\text{solv}} - H(e^-_{\text{gas}}) - H(\text{solvent}_{\text{solv}})$$

### 2.7.2 Calculation of reactions

The geometrical optimizations and frequency calculations were performed in gas-phase at the B3LYP [27,28]/6-31G (d, p) [29] level at 298.15 K. The ground states were confirmed to be real minima by frequency analysis (no imaginary frequency), while the transition states were determined by one imaginary frequency. Besides, IRC calculations [30, 31] were used to confirm that the transition structures properly connect the reactants and products. To obtain more reliable relative energies, single-point energy calculations for all optimized structures were carried at the M06-2X [32]/6-311+G (d, p) [33] in gas-phase at 298.15 K.

## 3. Results and discussions

### 3.1 Structural analysis of trisphenols and related phenols by X-ray diffractions and IR spectra.

#### Crystal structures

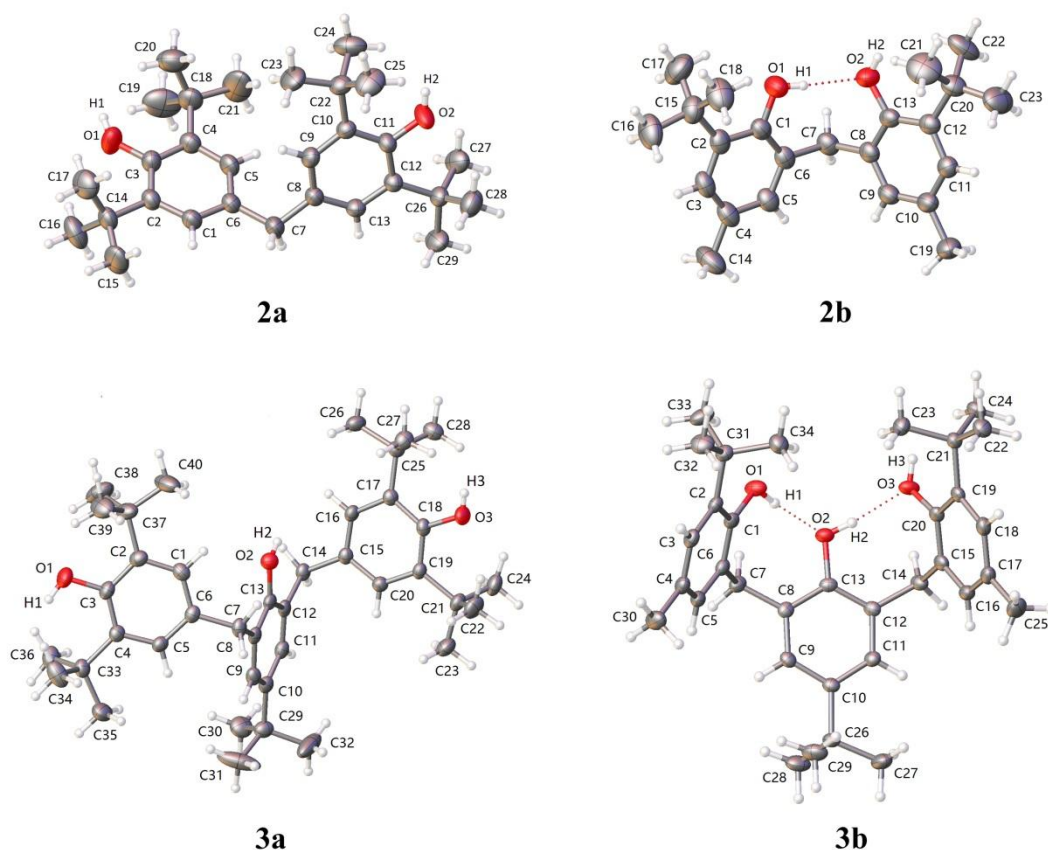


**Fig. 1.** X-ray crystal structures for bisphenols and trisphenols. Hydrogen bonds are shown as red dashed lines.

The structures of bisphenols and trisphenols were characterized by single crystal X-ray diffraction, shown in Fig. 1. Fig.2 provided their crystal packing diagrams. The crystal data and refinement details are given in Table 1 and Table 2 highlights important hydrogen bondings. Compound **2a** crystallizes in the centrosymmetric space group of the tetragonal system [34]. Two identical phenolic rings are linked by a “CH<sub>2</sub>” group which is located para to the OH groups on the arene rings. And each OH group, being nearly coplanar with the phenyl ring, is surrounded by two <sup>t</sup>Bu groups on its ortho-positions. The phenolic rings (C1/C6 and C8/C13) are twisted with an angle of 63.78° which can be considered as a result of intramolecular steric congestion between the two <sup>t</sup>Bu groups. No significant intermolecular hydrogen bonds,  $\pi$ - $\pi$  stacking or C-H $\cdots$  $\pi$  interactions are observed in the packing diagram due to the blocking from the bulky substituents.

**Table 1.** Crystal data and structure refinement for the bisphenols and trisphenols.

Identification code	<b>2a</b>	<b>2b</b>	<b>3a</b>	<b>3b</b>
Empirical formula	C <sub>29</sub> H <sub>44</sub> O <sub>2</sub>	C <sub>23</sub> H <sub>32</sub> O <sub>2</sub>	C <sub>40</sub> H <sub>58</sub> O <sub>3</sub>	C <sub>34</sub> H <sub>46</sub> O <sub>3</sub>
Formula weight	424.64	340.48	586.86	502.71
Temperature(K)	293(2)	293(2) K	130 K	130 K
Wavelength(Å)	0.71073	0.71073	0.71073	0.71073
Crystal system	Tetragonal	Orthorhombic	Triclinic	Monoclinic
Space group	I4 <sub>1</sub> /a	Pna21	P-1	P12 <sub>1</sub> /n1
a (Å)	21.1552(12)	16.105(2)	11.311(2)	14.7284(15)
b (Å)	21.1552(12)	12.7778(18)	12.387(3)	9.7166(10)
c (Å)	23.7623(17)	10.1418(15)	14.494(3)	21.691(2)
α(°)	90	90	112.184(4)	90
β(°)	90	90	102.014(4)	101.619(2)
λ(°)	90	90	94.922(4)	90
Volume (Å <sup>3</sup> )	10634.6(14)	2087.1(5)	1808.8(7)	3040.5(5)
Z	16	4	2	4
Density (calculated) (Mg/m <sup>3</sup> )	1.061	1.084	1.078	1.098
Absorption coefficient (mm <sup>-1</sup> )	0.064	0.067	0.066	0.068
Crystal size (mm <sup>3</sup> )	0.211 × 0.154 × 0.123	0.198 × 0.156 × 0.121	0.22 × 0.15 × 0.08	0.25 × 0.2 × 0.1
Index ranges	-26 ≤ h ≤ 26, -26 ≤ k ≤ 23, -26 ≤ l ≤ 29	-19 ≤ h ≤ 19, -15 ≤ k ≤ 15, -6 ≤ l ≤ 12	-14 ≤ h ≤ 16, -17 ≤ k ≤ 17, -20 ≤ l ≤ 20	-19 ≤ h ≤ 19, -13 ≤ k ≤ 12, -29 ≤ l ≤ 28
Reflections collected	32314	12194	18023	26644
Independent reflections	5243 [R(int) = 0.0556]	3072 [R(int) = 0.0353]	10838 [R(int) = 0.0612]	7882 [R(int) = 0.0452]
Final R indices [I > 2σ(I)]	R1 = 0.0513, wR2 = 0.1325	R1 = 0.0389, wR2 = 0.1048	R1 = 0.0673, wR2 = 0.1329	R1 = 0.0490, wR2 = 0.1148
R indices (all data)	R1 = 0.0815, wR2 = 0.1510	R1 = 0.0461, wR2 = 0.1101	R1 = 0.1951, wR2 = 0.1817	R1 = 0.0867, wR2 = 0.1329

**Table 2.** Selected hydrogen bondings for **2b** and **3b** (Å, °)

Compound	D-H...A	d(D-H)	d(H...A)	d(D...A)	<(DHA)
<b>2b</b>	O(1)-H(1)...O(2)	0.82	1.95	2.767(2)	172.4
	O(2)-H(2)...O(3)	0.84	1.91	2.7451(16)	170.9

However, compound **2b** crystallizes in the centrosymmetric space group of the orthorhombic system [34]. Two phenolic rings facing to each other with an angle of 118.06° are linked by a “CH<sub>2</sub>” group at the ortho-position of each OH group. The other ortho-position and the para-position of the OH group are substituted by a <sup>t</sup>Bu group and a Me group respectively. An intramolecular hydrogen bond apparently exists between O(1), H(1) and O(2) with an bond angle of 172.4°, resulting in the slightly deviating of the O1-H1 bond from the plane of the corresponding phenyl ring.

In addition, no intermolecular hydrogen bonds are found in the crystal packing diagram.

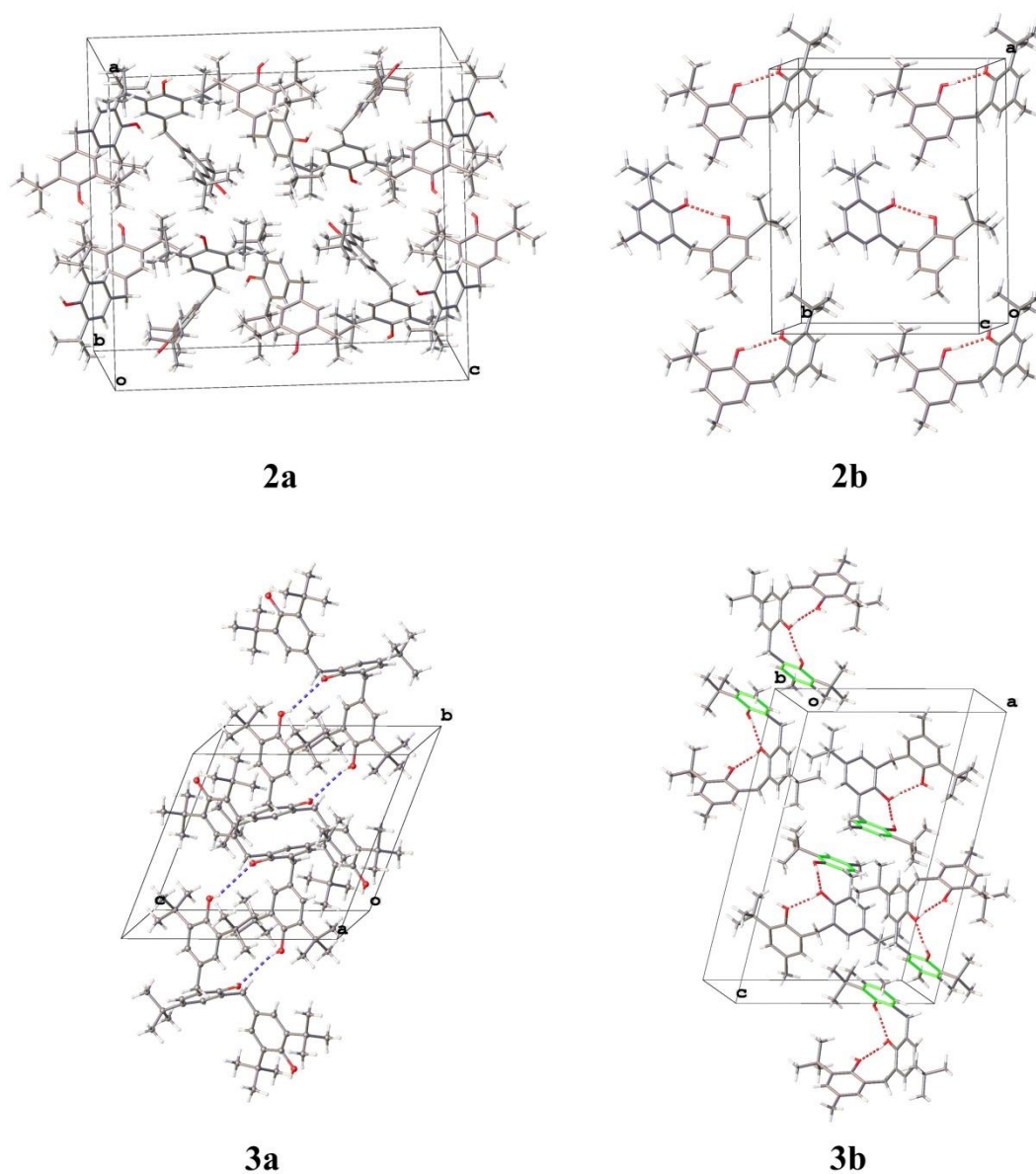


**Fig. 2.** The crystal packing diagrams for bisphenols and trisphenols. Intra- and intermolecular hydrogen bonds are shown as red and blue dashed lines respectively. The phenyl groups that generated  $\pi$ - $\pi$  stackings in **3b** are drawn in green.

Trisphenol **3a** containing three phenolic rings crystallizes in the triclinic space group P-1. Two ortho-positions of the OH group in the central phenolic ring are both linked with a phenolic ring through a “CH<sub>2</sub>” group. Both of the OH groups in the two side phenolic rings are located para to the central phenolic ring and encompassed by two

<sup>t</sup>Bu groups on their ortho-positions respectively, leading to the separation of the three OH groups. An S-shaped configuration is adopted with one outer aryl group situated above and one below the central phenolic group which can deeply reduce the steric hindrance. Two weak intermolecular hydrogen bonds are observed between the oxygen atom from the central phenolic ring of one compound and the hydrogen atom from the side phenolic ring of another one.

In the case of **3b**, the OH groups from three phenolic rings are neighboring and the oxygen atoms form a linear arrangement with two short separations of 2.7484(15) and 2.7451(16) Å between the central and outer oxygen atoms. Two intramolecular hydrogen bonds have been produced due to the proximity of these phenolic groups, resulting in a U-shaped configuration of the molecule. In the crystals, the side phenolic rings from two different molecules generate significantly face-to-face  $\pi$ - $\pi$  stackings in an offset manner and the formed dimers are isolated from each other.

### IR spectra

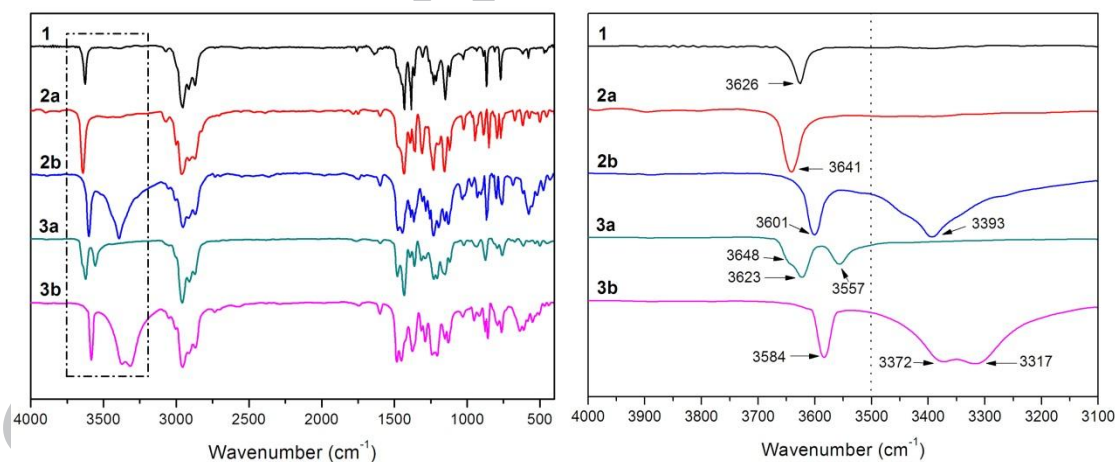


**Fig. 3.** Infrared spectra of the traditional antioxidants and the synthesized compounds.

The right picture is a large version of the figure in the left dotted box.

IR spectra of five phenols using KBr disc technique were provided in Fig. 3. The major differences of the five phenols in IR spectra are the peaks with the absorption above  $3000\text{ cm}^{-1}$  which are the characteristic peaks of OH groups. In the infrared spectra of BHT (**1**), significant signal is present at  $3626\text{ cm}^{-1}$  attributed to the free OH

group. **2a** containing two OH groups shows only a single sharp line characteristic of free OH centered at  $3641\text{ cm}^{-1}$ , similarly to BHT. It is remarkably demonstrated that the structure is symmetrical without any hydrogen interaction. However, **2b** shows two different hydroxyl absorptions including a sharp one ( $3601\text{ cm}^{-1}$ ) and a much broader one ( $3393\text{ cm}^{-1}$ ) which can be concluded that one is free OH group and the other is intramolecular hydrogen bonded, similarly to the reports [10]. In the infrared spectra of trisphenol **3a**, one signal at  $3623\text{ cm}^{-1}$  and a shoulder peak at  $3648\text{ cm}^{-1}$  are the characteristic peaks of free OH. The other OH peak appears at  $3557\text{ cm}^{-1}$  probably due to the weak intermolecular hydrogen bonding. For the case of **3b**, the peak at  $3584\text{ cm}^{-1}$  can be assigned to the free OH and two other broad ones between  $3300\text{ cm}^{-1}$  to  $3400\text{ cm}^{-1}$  are the OH groups that participate in the intramolecular hydrogen bonding. All the results are in a favorable consistence with that of the X-ray diffractions.

### 3.2 Thermal analysis under nitrogen or air

The thermal stabilities of the phenols were then investigated under nitrogen or air and the results are shown in Fig. 4 and Table 3.  $T_{\text{on}}$  and  $T_{\text{max}}$  are defined as the temperature at 5% weight loss and the temperature of maximum weight loss rate, respectively;  $\alpha_{\text{max}}$  is the maximum weight loss rate. The results of the thermal stability investigations under inert conditions, presented in Fig. 4a and 4b, showed that all of the antioxidants undergo weight loss over a single stage. The  $T_{\text{on}}$  and  $T_{\text{max}}$  of BHT are around  $91\text{ }^{\circ}\text{C}$  and  $138\text{ }^{\circ}\text{C}$ , respectively. Bisphenol **2a** provides a higher  $T_{\text{on}}$  ( $182\text{ }^{\circ}\text{C}$ ) and  $T_{\text{max}}$  ( $243\text{ }^{\circ}\text{C}$ ) than that of **2b** ( $177$  and  $239\text{ }^{\circ}\text{C}$ , respectively). Compared to the bisphenols, the thermal stabilities of trisphenols make a large improvement which provide a proximate  $T_{\text{on}}$  ( $245\text{ }^{\circ}\text{C}$ ) and  $T_{\text{max}}$  ( $310\text{ }^{\circ}\text{C}$ ). It should be noted that **3a** with a higher molecular weight exhibits almost identical thermal stability to that of **3b**. This is probably because the more numbers of the 'Bu group in **3a**'s structure would make it easier to take off small molecules while the intramolecular hydrogen bonds in **3b** may partly hinder the release of water.

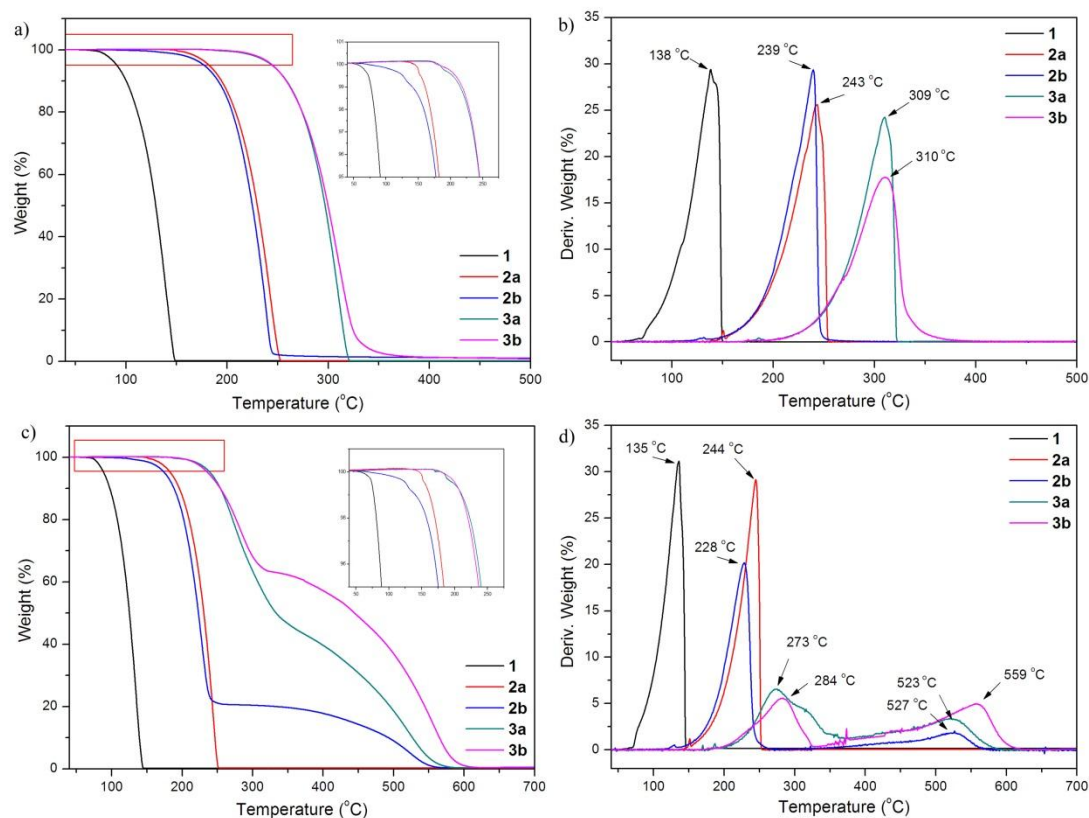


**Fig. 4.** TG and DTG curves of the traditional antioxidants and the synthesized compounds: (a) The TG curves under nitrogen; (b) The DTG curves under nitrogen; (c) The TG curves under air; (d) The DTG curves under air.

**Table 3.** Thermal decomposition data for the traditional antioxidants and the synthesized compounds

Samples		<b>1</b>	<b>2a</b>	<b>2b</b>	<b>3a</b>	<b>3b</b>
Molecular weight (g/mol)		235.19	424.67	340.50	586.89	502.73
Nitrogen	$T_{on}$ ( $^{\circ}C$ )	91	182	177	245	245
	$T_{max1}$ ( $^{\circ}C$ )	138	243	239	309	310
	$\alpha_{max1}$ (%/ $^{\circ}C$ )	2.852	2.495	2.206	2.376	1.768
Air	$T_{on}$ ( $^{\circ}C$ )	88	184	175	240	237
	$T_{max1}$ ( $^{\circ}C$ )	135	244	228	273	284
	$T_{max2}$ ( $^{\circ}C$ )	-	-	527	523	559
	$\alpha_{max1}$ (%/ $^{\circ}C$ )	2.994	2.811	1.987	0.651	0.553
	$\alpha_{max2}$ (%/ $^{\circ}C$ )	-	-	0.185	0.333	0.495

The thermo-oxidative stability under reactive conditions was also investigated, shown in Fig. 4c and 4d. Under air condition, **1** and **2a** have a single-step degradation progress but the other antioxidants have a two-step degradation progress which is different from the results under nitrogen. The first decomposition process of **2b**, **3a**

and **3b** occur between 200-300 °C probably induced by easily releasing of water and small molecules from the compounds. And at the higher temperature of this stage some stable intermediates may possibly be produced through the reaction with oxygen, leading to the second degradation step occurred at around 520-560 °C. It is worth noting that under air condition the trisphenols still behaved a much better thermo-oxidative stability than bisphenols and BHT although the  $T_{on}$  and  $T_{max1}$  exhibited a little decline compared to nitrogen atmosphere. All the above results demonstrate that the trisphenols are suitable to apply at elevated temperatures (>200 °C).

### 3.3 Antioxidant activity in lubricant base oil.

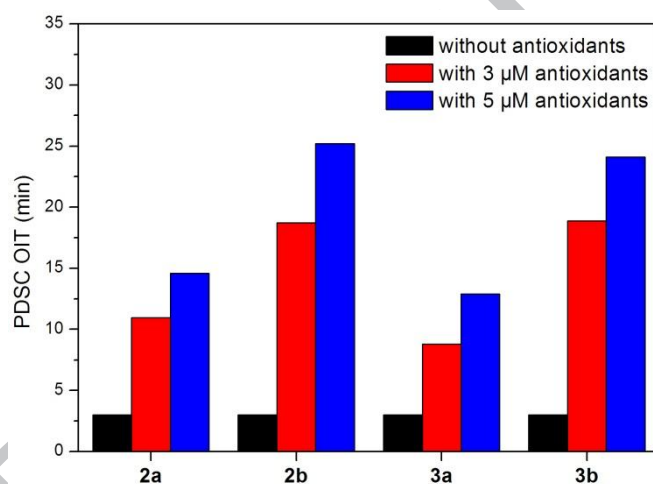


**Fig. 5** Comparison of the antioxidant activities between bisphenols and trisphenols in 150N in different concentrations using isothermal PDSC.

In order to investigate the actual antioxidant performance, bisphenols and trisphenols were added into lubricant base oils and their performance were tested using PDSC [35-37], shown in Fig. 5. In order to accelerate the autoxidation, the samples were heated at 180 °C where the pressure of oxygen was kept on 3.5 MPa during the test. The performance of compound **1** was not investigated due to its poor thermal stability under the test conditions. The oxidation process can be monitored by the exothermic situation. In the presence of antioxidants, the oxidation of base oil was inhibited without any energy loss of the system. Once the antioxidants were exhausted, base oil was quickly oxidized accompanied by the drastic heat release. Thus the antioxidant

activity can be evaluated by the oxidation induction time (OIT) which was measured from the start of the oxygen added in to the start of the exothermic peak. On adding of 3  $\mu\text{mol/g}$  different antioxidants, **3b** exhibited the highest OIT value of 18.87 min, followed by 18.73 min for **2b**, 10.95 min for **2a** and 8.81 min for **3a**. Compared with the pure oil, the OIT achieved a 5-fold increase for **2b** and **3b**, 2.6-fold increase for **2a** and 2-fold increase for **3a**. Increasing the concentration of the antioxidants to 5  $\mu\text{mol/g}$  afforded the OITs with a 7-fold increase for **2b** and **3b**, 3.9-fold increase for **2a** and 3.3-fold increase for **3a** compared with the pure oil. It is clearly indicated that those compounds containing the intramolecular hydrogen bonds (**2b** and **3b**) exhibited much better performance than others and their antioxidant activity have a larger improvement when increasing the concentration. Furthermore, it can be also found that at lower concentration **3b** performed a better activity than **2b**, while at higher concentration came out the opposite result. On the contrary, **3a** always exhibited the worst antioxidant activity of the four compounds.

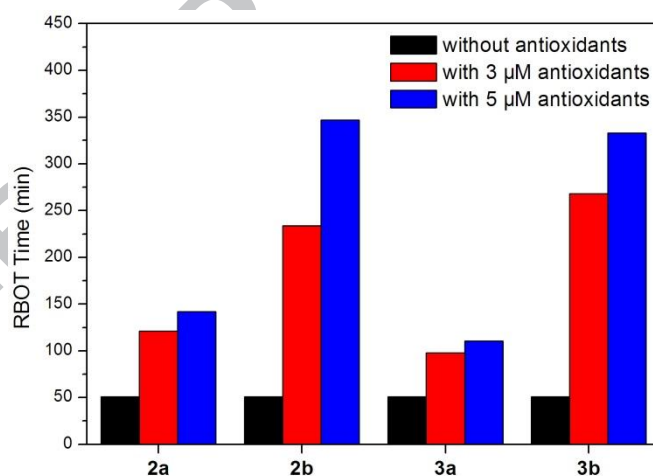


**Fig. 6** Comparison of the antioxidant activities between bisphenols and trisphenols in 150N in different concentrations using RBOT.

Except the high temperature and the pressure, metal ions and water are two of the most common factors that can accelerate the oxidation of oils in practice. Thus their antioxidant activities were also investigated in the presence of oxygen and catalyst (water and copper) using RBOT and the results are shown in Fig 6. The RBOT time of pure 150N is only 51 min. Adding of 3  $\mu\text{mol/g}$  antioxidants can enhance the RBOT

time with a 4.2-fold increase for **3b**, 3.5-fold increase for **2b**, 1.3-fold increase for **2a** and 0.9-fold increase for **3a**. Increasing the concentration of the antioxidants to 5  $\mu\text{mol/g}$  can largely improve the antioxidant activity for the oils containing **2b** and **3b**, but perform little influence for that of **2a** and **3a**. And the performance of **3b** became a little poorer than that of **2a**, different from when the concentration is 3  $\mu\text{mol/g}$ . In general, these phenols exhibited poorer activities in the RBOT tests than the PDSC tests which can be concluded that water and copper partly weakened the activity of the phenols during the antioxidation process. Nevertheless, the trend of the antioxidant activities has a good consistency with that of PDSC.

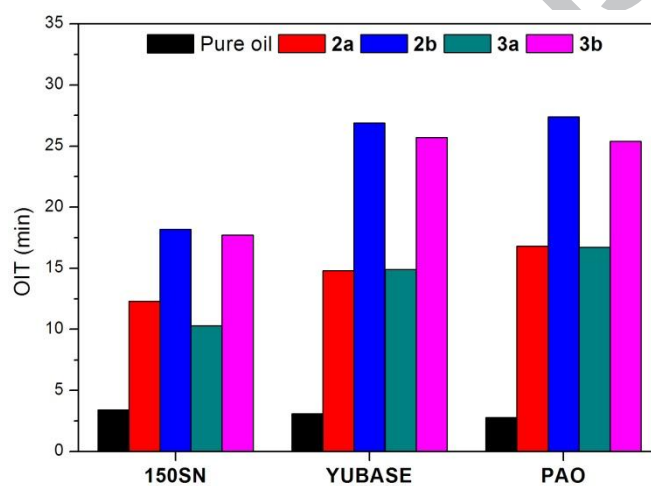


**Fig. 7.** Comparison of the antioxidant activities between bisphenols and trisphenols in other lubricant oils using isothermal PDSC.

Their antioxidant activity was further investigated in different base oils using isothermal PDSC. The oxidation induction times (OITs) containing 5  $\mu\text{mol/g}$  of various antioxidants are shown in Fig. 7. According to the American Petroleum Institute (API) [38], 150SN belonging to group I has less than 90% (m/m) saturates and more than 0.03% (m/m) sulfur. YUBASE (group III) are hydrogenated base oils containing more saturates ( $\geq 90\%$  m/m) and less sulfur ( $\leq 0.03\%$  m/m). Poly alpha olefin (PAO) is a kind of synthetic base oil, belonging to group IV. All of these phenolic compounds have good solubility in the three types of base oils and the solubility can be ranked as 150SN>YUBASE>PAO which can be concluded that a lower level base oil is accompanied by a better solubility of the phenols. Bisphenols

show better solubility than trisphenols but they were totally dissolved during the whole test. The OITs of the base oils themselves without any antioxidants are all less than 4 min. In contrast, after adding phenols to these oils, the OITs achieved 2.6 to 5-fold increase for **2a**, 4.3 to 8.7-fold increase for **2b**, 2.0 to 5-fold increase for **3a** and 4.2 to 8.0-fold increase for **3b**. They both obtained the best antioxidant efficiency in PAO but the worst in 150SN since more unsaturates that easier to autoxidize are contained in 150SN. In all the base oils, the antioxidant activities can be ranked as **2b**>**3b**>**2a**>**3a**, similarly to the results above.

### 3.4 DFT calculations

#### 3.4.1 Calculations of BDE and IP

**Table 4.** Calculated BDE and IP values of the most stable isomers in the gas phase and *n*-hexane.

Calculative content	Solvent	<b>2a</b>	<b>2b</b>	<b>3a</b>	<b>3b</b>
BDE (kcal•mol <sup>-1</sup> )	Gas phase	76.16	74.94	75.61	75.30
	<i>n</i> -hexane	77.43	74.27	76.98	73.89
IP (kcal•mol <sup>-1</sup> )	Gas phase	168.30	165.97	166.44	162.40
	<i>n</i> -hexane	154.51	149.39	154.04	146.13

To study the radical scavenging activities of phenols as antioxidants, thermodynamic properties consisting of bond dissociation enthalpy (BDE) and ionization potential (IP) values in gas-phase and *n*-hexane (the solvent which was performed in the experiment) were calculated and the results are shown in table 4. Fig. 8 presents the most stable configurations of the formed phenolic radicals. In general, the highly effective antioxidants have relatively low BDE and IP values. The BDE calculation is on the base of a HAT mechanism which evaluates the easiness of the homolytic cleavage of the bond [39]. In the gas phase two of the O-H groups in compound **2a** are identical with the same BDE values of 77.43 kcal•mol<sup>-1</sup>. The most active O-H group for **2b**, **3a** and **3b** is the free one without any inter- or intra-molecular hydrogen bonding and the BDE values are 74.27 kcal•mol<sup>-1</sup>, 75.61 kcal•mol<sup>-1</sup> and 73.89 kcal•mol<sup>-1</sup> respectively. In *n*-hexane, the BDE values of **2a** and **3a** increase with about 1.3 kcal•mol<sup>-1</sup> while the values of **2b** and **3b** decrease with 0.67 and 1.41 kcal•mol<sup>-1</sup> respectively. The

increasing wide gaps of the BDE values of the four phenols obviously show that the O-H groups of **2b** and **3b** become more active than that of **2a** and **3a** in nonpolar solvent, verifying the better antioxidant performance of **2b** and **3b** in the lubricant oils since most of the compositions in oils are hydrocarbon compounds.

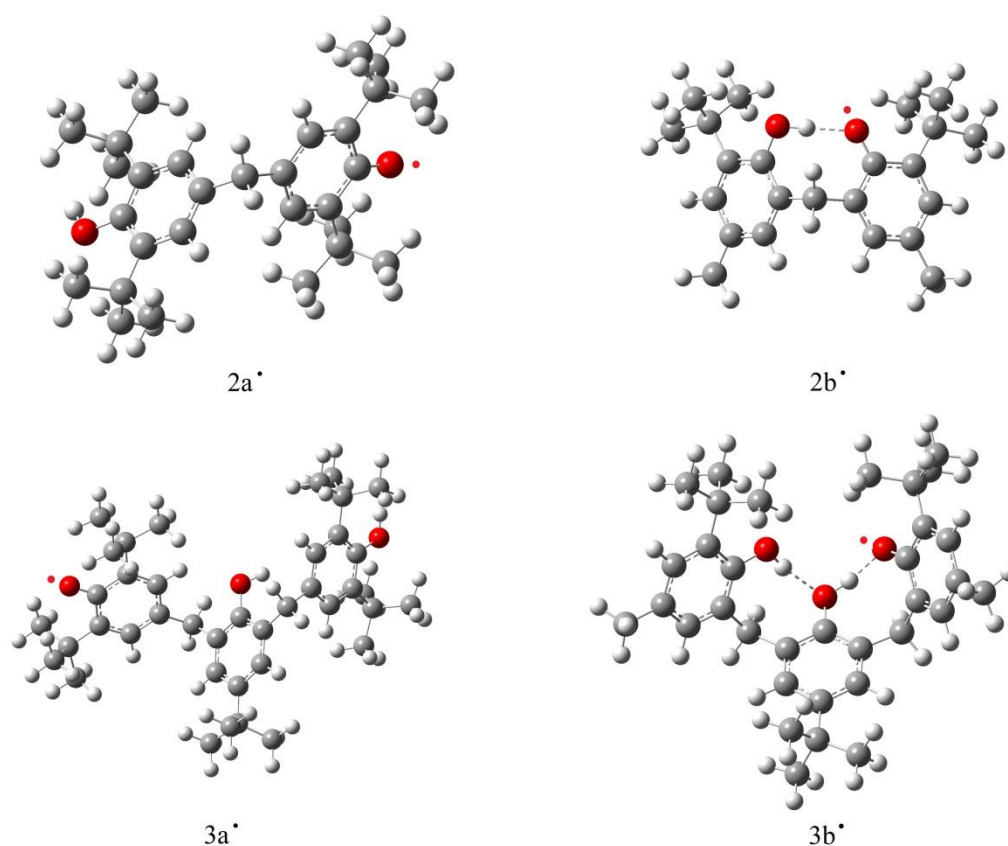
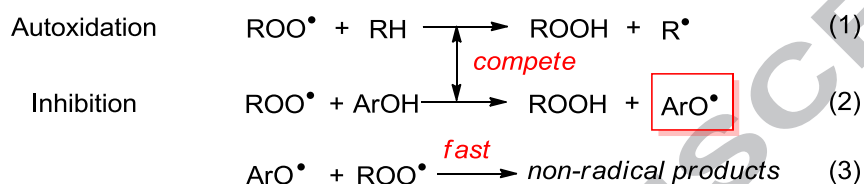


**Fig 8.** The most stable configurations of the formed phenolic radicals.

The IP calculation undergoes the SET-PT mechanism including the process of losing one electron to generate a radical cation and the following deprotonating of the radical cation to create the corresponding radical [40]. Thus the IP values illustrate the easiness of electron donation of phenolic compounds. In the gas phase, **3b** shows the lowest IP value of  $162.4 \text{ kcal}\cdot\text{mol}^{-1}$ , followed by **2a** of  $165.97 \text{ kcal}\cdot\text{mol}^{-1}$ , **3a** of  $166.44 \text{ kcal}\cdot\text{mol}^{-1}$  and **2a** of  $168.30 \text{ kcal}\cdot\text{mol}^{-1}$ . While in *n*-hexane, a decrease of about  $12\text{-}14 \text{ kcal}\cdot\text{mol}^{-1}$  have been observed for the IP values of all the phenols which are quite larger than the variations of BDE values, obviously demonstrating that the

electron transfer process is more sensitive to the solvent. Nevertheless, both of BDE and IP values of **2b** and **3b** in gas-phase and *n*-hexane are lower than that of other compounds which indicates that **2b** and **3b** have higher antioxidant activities.

### 3.4.2 Calculations of the TS structures and the energy barriers for the reaction of the antioxidants and alkyl peroxy radicals



**Scheme 4.** Oxidation mechanism in oils.

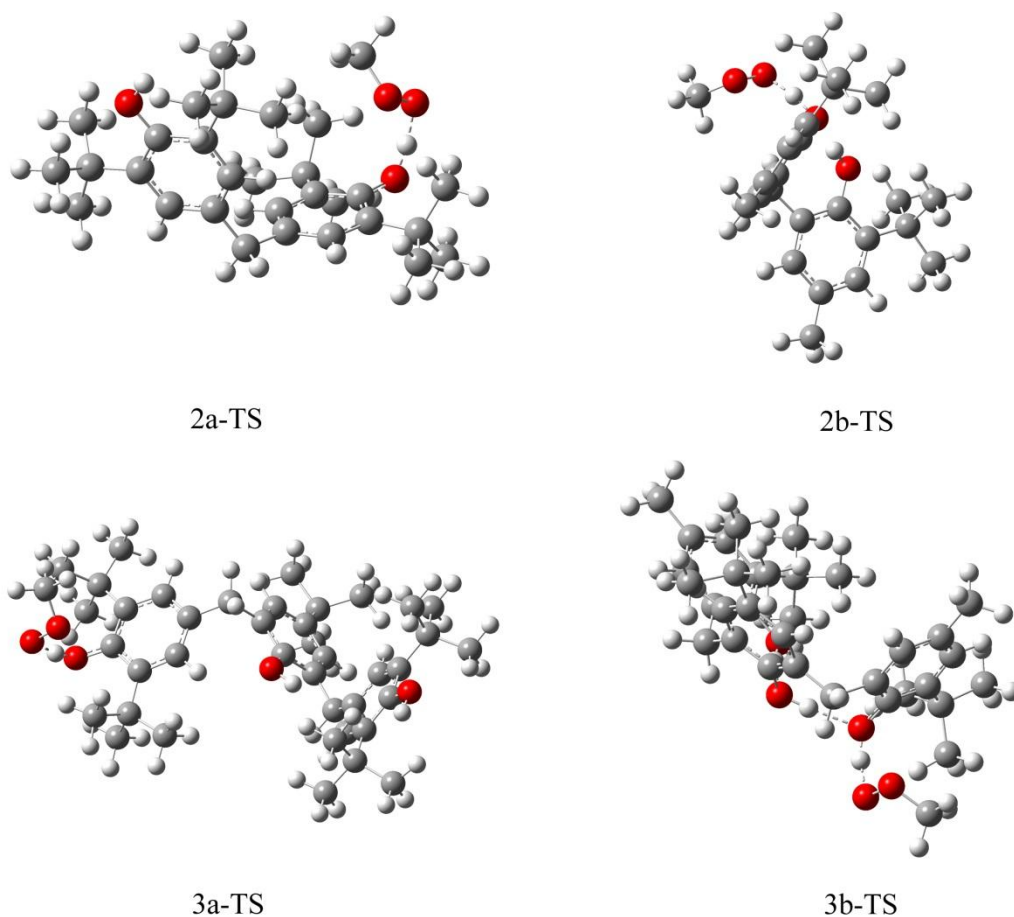


**Fig. 9.** Calculated TS structures for the reaction between phenols and a methylperoxyl radical.

During the oxidation of base oil (Scheme 4), alkyl peroxy radical ( $\text{ROO}^\bullet$ ) was the most pernicious radical which can quickly abstract hydrogen from hydrocarbon molecule to accelerate the degradation of base oil (eq 1) [41]. In this regard, phenols acted as the radical scavengers donated hydrogen atoms to terminate  $\text{ROO}^\bullet$  to afford hydroperoxides ( $\text{ROOH}$ ) (eq 2) and the obtained phenoxy radicals can rapidly react with another  $\text{ROO}^\bullet$  to afford non-radical compounds (eq 3). Thus the inherent antioxidant efficacies of the phenols can be evaluated by the reactivity with peroxy radicals since it is the reaction that competes with the rate-determining step of oxidation [42-43]. In consequence, the TS structures and the energy barriers of the inhibited step were calculated by DFT methods, shown in Fig. 9 and Fig. 10. This step undergo a proton coupled electron transfer (PCET) mechanism including proton transfer perpendicularly to the phenolic ring, together with electron transfer from a lone pair on the oxygen of phenol to the radical. Compound **2b** and **3b** provide the lowest Gibbs free energy of this step with 13.52 and 13.87 kcal/mol respectively, followed by **2a** (16.85 kcal/mol) and **3a** (16.98 kcal/mol). The TS structures show that the less bulky of “ $\text{CH}_2$ ” substituents on the *o*-position of O-H group in **2b** and **3b** make it easier for the approach of  $\text{MeOO}^\bullet$  to the hydroxyl hydrogen. Interestingly, in the TS of the four compounds, a syn arrangement of phenols and methylperoxy radical is preferred, afforded an additional overlap between 2p lone pairs on the inner O-atom of  $\text{MeOO}^\bullet$  and the  $\pi$  electros of the phenolic rings which can further stabilize the transition state [44-46]. Furthermore, it should be noted that the stabilization of the formed phenoxy radical has also an important influence on the activities [10, 47]. The calculations show that the most stable configurations of **2b** $^\bullet$  and **3b** $^\bullet$  can be further stabilized by the remained intramolecular hydrogen bonding which can additionally accelerate the rate of eq. 2 (Fig. 8). In short, the less bulky substituents of the substrate, the additional stabilization of the transition state and the more stabilization of the generated phenolic radical simultaneously give rise to the higher antioxidant activity of compound **2a** and **3b**. These calculations provided a favorable consistency with the experimental results.

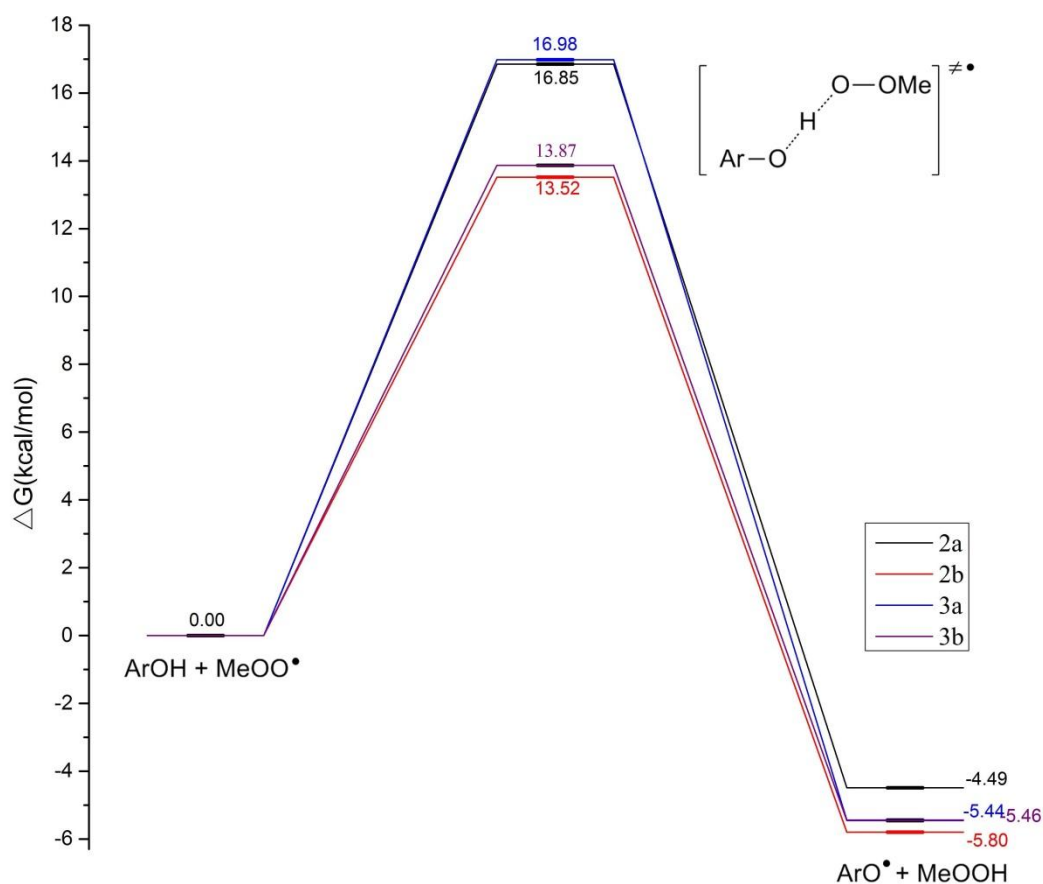


**Fig. 10.** The calculated free energy barriers for the reaction between phenols and a methylperoxyl radical.

#### 4 Conclusions

We have successfully synthesized two types of trisphenols bridged by two “CH<sub>2</sub>” groups in different ways. The X-ray diffractions and IR spectra showed that **3a** has an S-shaped configuration with intermolecular hydrogen bonds while **3b** presents a U-shaped configuration with two intramolecular hydrogen bonds. They both showed better thermal stability than the traditional ones in nitrogen or air due to their higher molecular weight. When adding them into lubricant oil, compound **3b** exhibited the best antioxidant activity, nearly identical to that of **2b**, while **3a** performed the worst. The computational results showed that **3b** provides the lowest BDE and IP values while **3a** gives the highest results. Furthermore, the calculations for the reaction with alkyl peroxy radicals showed that the superior performance of **3b** is due to three factors including the less bulky substituents of the substrate, the additional

stabilization of the transition state from the overlap between 2p lone pairs and the  $\pi$  electrons, and the more stabilization of the generated phenolic radical ascribed to the two strong intramolecular hydrogen bonds.

### Acknowledgements

We thank Professor Shuzhou Li, School of Materials Science and Engineering Nanyang Technological University in Singapore, for providing helpful idea and thoughts about the computation. This work was supported by “Thousand Talents Program”, National Natural Science Foundation of China (Grand No. 21606247), China Postdoctoral Science Foundation (Grand No. 2016M590555), Zhejiang Postdoctoral Sustentation Fund, China (Grand No. BSH1502163) and the Natural Science Foundation of Ningbo (Grand No. 2016A610260).

### References

- [1] R. Czochara, J. Kusio, M. Symonowicz, G. Litwinienko, *Ind. Eng. Chem. Res.* 55 (2016) 9887.
- [2] L. T. Zhang, G. X. Cai, W. M. J. Eli, *Lubr. Sci.* 25 (2013) 209.
- [3] Kumar, A. *Antioxidants Applications and Global Markets*, BCC Research, Mar. 2015.
- [4] W. A. Yehye, N. A. Rahman, A. Ariffin, S. B. A. Hamid, A. A. Alhadi, F. A. Kadir, M. Yaeghoobi, *Eur. J. Med. Chem.* 101 (2015) 295.
- [5] W. Wang, P. Kannan, J. Xue, K. Kannan, *Environ. Res.*, 151 (2016) 339.
- [6] Y. Bolbukh, P. Kuzema, V. Tertykh, I. Laguta, *J. Therm. Anal. Calorim.* 94 (2008) 727.
- [7] R. Gensler, C. J. G. Plummer, H. H. Kausch, E. Kramer, J. R. Pauquet, H. Zweifel, *Polym. Degrad. Stab.* 67 (2000) 195.
- [8] A. Yano, S. Watanabe, Y. Miyazaki, M. Tsuchiya, Y. Yamamoto, *Tribol Trans.* 47 (2004) 111.
- [9] S. Yu, J. X. Feng, T. Cai, S. G. Liu, *Ind. Eng. Chem. Res.* 56 (2017) 4196.
- [10] R. Amorati, M. Lucarini, V. Mugnaini, G. F. Pedulli, *J. Org. Chem.* 68 (2003) 5198.

- [11] M. Lucarini, G. F. Pedulli, L. Valgimigli, R. Amorati, *J. Org. Chem.* 66 (2001) 5456.
- [12] R. Amorati, J. Zotova, A. Baschieri, L. Valgimigli, *J. Org. Chem.* 80 (2015) 10651.
- [13] M. Ogata, M. Hoshi, K. Shimotohno, S. Urano, T. Endo, *J. Am. Oil Chem. Soc.* 74 (1997) 557.
- [14] C. Zhao, Z. -Q. Liu, *Biochimie.* 93 (2011) 1755.
- [15] S. Dikalov, T. Losik, J. L. Arbiser, *Biochem. Pharmacol.* 76 (2008) 589.
- [16] Gaussian 09, Revision A.1, M. J. Frisch, G. W. Trucks, H. B. Schlegel, G. E. Scuseria, M. A. Robb, J. R. Cheeseman, G. Scalmani, V. Barone, B. Mennucci, G. A. Petersson, H. Nakatsuji, M. Caricato, X. Li, H. P. Hratchian, A. F. Izmaylov, J. Bloino, G. Zheng, J. L. Sonnenberg, M. Hada, M. Ehara, K. Toyota, R. Fukuda, J. Hasegawa, M. Ishida, T. Nakajima, Y. Honda, O. Kitao, H. Nakai, T. Vreven, J. A. Montgomery, Jr., J. E. Peralta, F. Ogliaro, M. Bearpark, J. J. Heyd, E. Brothers, K. N. Kudin, V. N. Staroverov, R. Kobayashi, J. Normand, K. Raghavachari, A. Rendell, J. C. Burant, S. S. Iyengar, J. Tomasi, M. Cossi, N. Rega, J. M. Millam, M. Klene, J. E. Knox, J. B. Cross, V. Bakken, C. Adamo, J. Jaramillo, R. Gomperts, R. E. Stratmann, O. Yazyev, A. J. Austin, R. Cammi, C. Pomelli, J. W. Ochterski, R. L. Martin, K. Morokuma, V. G. Zakrzewski, G. A. Voth, P. Salvador, J. J. Dannenberg, S. Dapprich, A. D. Daniels, Ö. Farkas, J. B. Foresman, J. V. Ortiz, J. Cioslowski, and D. J. Fox, Gaussian, Inc., Wallingford CT, 2009.
- [17] Gaussview Rev. 3.09, Windows version. Gaussian Inc., Pittsburgh.
- [18] J. Tomasi, B. Mennucci, E. Cancès, *J. Mol. Struct. Theochem.* 464 (1999) 211.
- [19] J. S. Wright, E. R. Johnson, G. A. DiLabio, *J. Am. Chem. Soc.* 123 (2001) 1173.
- [20] J. E. Bartmess, *J. Phys. Chem.* 98 (1994) 6420.
- [21] M. M. Bizarro, B. J. C. Cabral, R. M. B. Santos, J. A. M. Simões, *Pure Appl. Chem.* 71 (1999) 1249.
- [22] W. D. Parker, *J. Am. Chem. Soc.* 114 (1992) 7458.
- [23] E. Wilhelm, R. Battino, *Chem. Rev.* 73 (1977) 1.
- [24] Z. Marković, J. Tošović, D. Milenković, S. Marković, *Comput. Theor. Chem.*

1077 (2016) 11.

[25] J. J. Fifen, M. Nsangou, Z. Dhaouadi, O. Motapon, N. Jaidane, *Comput. Theor. Chem.* 966 (2011) 232.

[26] J. Rimarčík, V. Lukeš, E. Klein, M. Ilčin, *J. Mol. Struct. (Theochem)* 952 (2010) 25.

[27] A. D. Becke, *J. Chem. Phys.* 98 (1993) 5648

[28] P. J. Stephens, F. J. Devlin, C. F. Chabalowski, M. J. Frisch, *J. Chem. Phys.* 98 (1994) 11623

[29] P. C. Hariharan, J. A. Pople, *Theor. Chim. Acta.* 28 (1973) 213.

[30] K. Fukui, *J Phys Chem* 74 (1970) 4161.

[31] K. Fukui, *Acc Chem Res.* 14 (1981) 363.

[32] Y. Zhao, D. G. Truhlar, *Theor. Chem. Account.* 120 (2008) 215.

[33] A. D. McLean, G. S. Chandler, *J. Chem. Phys.* 72 (1980) 5639.

[34] Compound **2a** and **2b** has already been reported in previous literatures. We discussed their crystal structures here in order to better understand the relationship between structures and properties of different phenols. For **2a**, please see: T. J. Boyle, L. A. M. Steele, D. T. Yonemoto, *J. Coord. Chem.* 65 (2012) 487. For **2b**, please see: L. A. Chetkina, V. E. Zavodnik, V. K. Bel'skii, I. G. Arzamanova, M. I. Naiman, and Ya. A. Gurvich, *J. Struct. Chem.* 25 (1985) 935.

[35] C. Qiu, S. Han, X. Cheng, T. Ren, *Thermochimica Acta* 447 (2006) 36.

[36] C. Miao, Y. Zhang, G. Yang, S. Zhang, L. Yu, P. Zhang, *Ind. Eng. Chem. Res.* 55 (2016) 12703.

[37] C. Miao, D. Yu, L. Huang, S. Zhang, L. Yu, P. Zhang, *Ind. Eng. Chem. Res.* 55 (2016) 1819.

[38] *Engine Oil Licensing and Certification System*, 17th ed.; API Publication 1509; American Petroleum Institute, September 2015.

[39] Y. Zhao, N. E. Schultz, D. G. Truhlar, *J. Chem. Phys.* 123 (2005) 161103.

[40] Z. Marković, D. Amić, D. Milenković, J. M. D. Marković, S. Marković, *Phys. Chem. Chem. Phys.* 15 (2013) 7370.

- [41] J. Dong, C. A. Migdal, Antioxidants. In *Lubricant Additives: Chemistry and Application*, 2nd ed; Rudnick, L. R. Ed.; CRC Press: Boca Raton, 2009; pp 3-50.
- [42] B. Li, J. R. Harjani, N. S. Cormier, H. Madarati, J. Atkinson, G. Cosa, D. A. Pratt, *J. Am. Chem. Soc.* 135 (2013) 1394.
- [43] G. W. Burton, K. U. Ingold, *Acc. Chem. Res.* 19 (1986) 194.
- [44] G. A. DiLabio, K. U. Ingold, *J. Am. Chem. Soc.* 127 (2005) 6693.
- [45] G. A. DiLabio, E. R. Johnson, *J. Am. Chem. Soc.* 129 (2007) 6199.
- [46] L. Valgimigli, R. Amorati, S. Petrucci, G. F. Pedulli, D. Hu, J. J. Hanthorn, D. A. Pratt, *Angew. Chem., Int. Ed.* 48 (2009) 8348.
- [47] P. J. O'Malley, *J. Phys. Chem. B* 106 (2002) 12331.

## Highlights

- Synthesis and characterization of two new type trisphenols
- Superior thermal stability and highly antioxidant efficiency of the synthesized compounds in lubricant oils compared to the related phenols
- The relationship between structure and properties explored by a series of DFT calculations